Mechanics of Energy Absorbability in Plain-Woven Fabrics: An Analytical Approach

Ali M. Sadegh[1], Paul V. Cavallaro[2]

[1]The City College of The City University of New York, New York, New York UNITED STATES

[2]Naval Undersea Warfare Center Division, Newport, Rhode Island UNITED STATES

Correspondence to:
Ali Sadegh email: sadegh@ccny.cuny.edu

ABSTRACT:
Experimental studies have shown that flexible woven fabrics can absorb significant kinetic energy from both projectile and fragment impacts through a combination of design factors which include yarn materials, weaving architectures, yarn density ratios, as well as the projectile mass, shape and velocity.[1-3] This paper investigates the relationships between various plain-woven fabric architectures, crimp imbalance and energy absorption capacities when rigid projectile strike these fabrics through a series of analytical solutions. This was accomplished through formulations of the yarn pullout and yarn migration forces. Special attention is given to the friction forces generated between yarn families at the yarn crossover regions. It was assumed that the yarns do not fail while the projectile penetrates through the fabric. Finally, the relationships between the residual velocities of the projectile and the contact angles α, (that is, the angle of circumferential contact between crossing yarns which is related to the crimp content) were determined. The results indicated that for ballistic impacts, highly crimp-imbalanced woven fabrics perform in a manner far superior to that of equally-crimped woven fabrics. These analytical solutions resulted in the ability to parametrically study the effects of crimp contents and, in particular, crimp imbalance on the effectiveness of plain-woven fabric armors.

NOMENCLATURE:

D	Projectile diameter
D_x	Yarn migration distance in x-direction
D_y	Yarn migration distance in y-direction
F_i	Projectile force on an individual yarn
h	Distance between centerlines of adjacent crossover regions in HCC direction
HCC	High crimp content yarn
LCC	Low crimp content yarn
n	Number of crossover regions
N	Newton
P	$P = R/T_n$
r	Radius of yarn cross-section
R	Yarn migration force
t	Distance between centerlines of adjacent crossover regions in LCC direction
T_i	Yarn pullout (tension) force
T_n	Tension at clamped side of fabric
V_1	Initial velocity of projectile
V_2	Residual velocity of projectile
ω	Uniform load per unit length
μ	Coefficient of friction
α	Contact angle of yarns at crossover regions
θ	Circumferential contact angle
δ	Deflection of fabric
Δ_x	Yarn pullout distance in x-direction
Δ_y	Yarn pullout distance in y-direction

INTRODUCTION:
Flexible woven and unidirectional fabrics remain outstanding material systems for lightweight protection against ballistic and fragment impacts. Because of their heterogeneous constructions on multiple scales, these fabrics can absorb significant kinetic energy from projectile and fragment impacts through a combination of design factors which include yarn materials, weaving architectures, yarn density ratios (that is, the ratio of yarn counts per unit length), as well as projectile mass, shape, and velocity.[1-3] The mechanisms responsible for energy absorbability in plain-woven fabrics include yarn friction, crimp interchange, yarn stretching, yarn migration, fabric shearing, yarn pullout, and yarn breakage.[4,5] While the mechanisms of energy absorbability in woven fabrics have been recognized, their relationships to ballistic protection levels have not been fully quantified in the open literature. The authors' previous findings demonstrated that crimp imbalance (defined as the ratio of crimp contents among yarn directions) had substantial influence on the energy absorption levels of single-ply, plain-woven fabrics[6]. This current investigation, an

extension of their earlier research, describes a series of analytical models developed to establish the relationship between crimp imbalance and the energy absorbability of plain-woven fabrics subjected to ballistic impact.

Contrary to the intuitive belief that tightly woven and equally crimped (also referred to as "iso-crimped") fabrics perform well in ballistic impacts, it has been argued and demonstrated that highly crimp-imbalanced plain-woven fabrics can perform in a manner far superior to iso-crimped plain-woven fabrics.[6] The current research analytically investigates the validity of such a claim. Specifically, this work focuses on energy absorption of plain-woven fabrics (that is, the reduction of projectile velocity upon impact) as a function of the contact angle α (that is, the angle of circumferential contact between crossing yarns). Note that the magnitude of α constitutes the crimp ratio and the crimp imbalance.

Forces due to projectile impacts can be classified into two categories: high-velocity impacts and low-velocity impacts. In high-velocity ballistic impacts where the projectile velocity exceeds 300 m/sec, the yarns may fail prior to the occurrence of yarn migration as demonstrated by plug-type failures observed in experimental tests. In this study the impact velocity of the projectile is considered to be within the low-velocity regime and it is assumed that yarns do not fail; rather, they are permitted to migrate with respect to each other.

In low-velocity ballistic impacts, a plain-woven fabric may absorb the projectile's kinetic energy through the following sequential phenomena: (1) the projectile creates a conical depression on the plane of the fabric upon initial contact; (2) the yarns in direct contact with the projectile (referred to as "primary yarns") are subjected to tension, and, at the crossover regions where yarn families intersect, friction and shearing deformations develop; and (3) primary yarns begin to migrate away from the projectile contact region and initiate an opening. This sequence of events can be sufficient to create openings, enabling the projectile to penetrate the fabric without yarn failure. The energy absorbed by the fabric is dependent upon the projectile mass and velocity, impact force, fabric architecture, yarn construction and material properties of the fibers used.

Prior to this study, the influence of yarn crimp on the ballistic impact resistance of plain-woven fabrics had neither been sufficiently addressed nor adequately understood; the open literature lacked conclusive research findings relating yarn crimp to energy absorption levels.

The primary objectives of this research were to: (1) investigate the projectile penetration mechanisms in single-ply, plain-woven fabrics, (2) develop analytical formulations of yarn pullout and yarn migration forces, (3) determine the work required to create openings between yarns through yarn migration and (4) determine the energy absorbed by a projectile when it passes through these openings. The results indicated that crimp imbalance (which exists when the ratio of crimp contents among yarn directions is other than unity) had substantial influence on the energy absorption levels of plain-woven fabrics.

Specifically, this research investigates the energy absorbability of crimp-imbalanced protective (*CRIMP*) plain-woven fabrics when subjected to ballistic impact forces. Specific areas of investigation include (1) a closed-form approach to analytically investigate the associated parametric effects of crimp contents and yarn-yarn friction on the energy absorbability in plain-woven fabrics, (2) plain-woven fabric architectures, (3) yarn migration, (4) yarn pullout, and (5) energy absorption and projectile residual velocity.

The results of this study indicate that, for ballistic impacts in single-ply, plain-woven fabrics, the performance of highly crimp-imbalanced architectures were superior to those of tightly woven crimp-balanced architectures. The analytical solutions provide the means to parametrically quantify the effects of crimp imbalance on the protection levels of fabric armor materials.

In section 2, the yarn friction phenomenon is discussed which is followed by the formulation of the yarn pullout forces in section 3. Yarn migration and the forces required to separate yarns at the crossover regions are formulated in section 4. The total force required for a projectile to fully penetrate a fabric swatch, the energy absorption and the residual velocity of the projectile are calculated in sections 5 and 6, respectively. Finally, the results and conclusions are discussed in section 7. Due to the variety of section examples, the results of each section are provided in their specific section.

YARN FRICTION PHENOMENON:

The mechanics of energy absorbability in plain-woven fabrics, involves yarn decrimping, yarn

stretching, yarn migration, and yarn pullout. The forces required for yarn migration and pullout are related to the frictional properties of the yarns and the weaving architectures. The ballistic protection levels of plain-woven fabrics can be greatly altered, and often enhanced, by modifications to the frictional properties at both the fiber and yarn levels.[7-9] When a projectile comes in contact with the fabric, first, the frictional force between the projectile and the fabric is generated. This force is negligible for metallic plates, as demonstrated by the experimental work of Awerbuch and Bodner[10] and is assumed to be negligible in the fabric case. Second, the frictional force resulting from contact between crossing yarns plays an important role in the energy absorbability of the fabric.

Friction At The Crossover Regions:

When a projectile comes in contact with a woven fabric, it applies a contact force over several crossover regions. Consider a crossover region subjected to a contact force as shown in *Figure 1*.

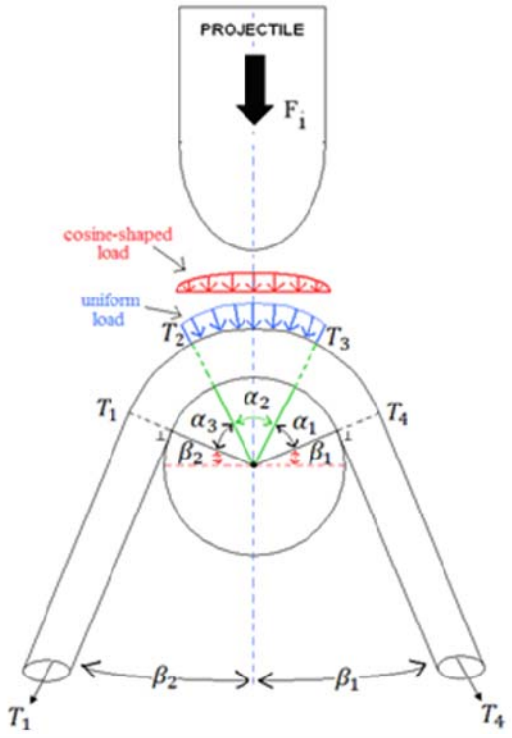

FIGURE 1. Projectile Force and Geometry at a Crossover Region (Uniform and Cosine-Shaped Loads)

The contact force creates three distinct sectors on the crossover region: α_1, α_2, and α_3. Note that α_2 is the sector where the projectile contacts the crossover yarn while α_1 and α_3 are the angles associated with the yarn-to-yarn contact. Let $\alpha = \alpha_1 + \alpha_2 + \alpha_3$. Two angles β_1 and β_2 were introduced so that $\beta_1 + \alpha_1 + \alpha_2 + \alpha_3 + \beta_2 = 180°$. Because of the symmetric loading of the crown of the crossover region, $\alpha_1 = \alpha_3$ and $\beta_1 = \beta_2$. Note that $\beta_1 = \beta_2 = \frac{180 - \alpha}{2}$. Although α_1 and α_3 and β_1 and β_2 are small compared to α_2, the yarn tensions on sectors α_1 and α_3 are nevertheless denoted as T_3 and T_2, respectively, which are different values than those of T_1 and T_4. When $\alpha_1 = \alpha_3 = 0$, then $T_3 = T_4$ and $T_1 = T_2$.

Depending on the shape of the leading surface of the projectile, the contact force between the projectile and the yarn at a crossover could be described, for example, by a uniformly distributed load or a cosine-shaped distributed load.

Uniformly Distributed Load

Consider a uniformly distributed load, ω, per unit length that expands over the angle α_2 (*Figure* 1). The total applied force to the i^{th} crossover region is denoted by $F_i = \omega r \alpha_2$, where r is the radius of the yarn. Three contact sections exist along the crossing yarn. The first and the third contact regions over the sectors α_1 and α_3 are governed by the basic friction equation $\frac{T_i}{T_{i+1}} = e^{\mu\alpha_i}$, for $i = 1$ or 3 and where μ is the coefficient of friction of yarn on yarn. The second contact region over sector α_2 was derived and is given by Eq. (1b). Solving the coupled Eq. (1a), Eq. (1b) and Eq. (1c) the ratio of T_1/T_4 can be calculated.

$$\frac{T_1}{T_2} = e^{\mu\alpha_1} \tag{1a}$$

$$\frac{T_2 + \frac{F_i}{\alpha_2}}{T_3 + \frac{F_i}{\alpha_2}} = e^{\mu\alpha_2} \tag{1b}$$

$$\frac{T_3}{T_4} = e^{\mu\alpha_3} \tag{1c}$$

Cosine-Shaped Distributed Load

For the i^{th} crossover region, consider the projectile force to be a cosine-shaped distributed load that varies over the angle of α_2 and is given by $F_i = a\cos\theta$ (*Figure 1*), where a is a constant and $0 < \theta < \alpha_2$. Similar to the uniformly distributed load case, there

are three contact regions along the crossing yarn. The first and the third contact regions reside over sectors α_1 and α_3 and are governed by the basic friction equation and are represented in Eq. (1a) and Eq. (1c), respectively. The tension on the second contact region, T_2, over sector α_2 was derived and is given by Eq. (2). By solving the coupled Eq. (1a), Eq. (1c) and Eq. (2) the ratio of T_1/T_4 for the cosine-shaped load can be calculated.

$$T_2 = \frac{2\mu a}{1+\mu^2}\sin\left(\frac{\alpha_2}{2}\right) + ce^{\mu\alpha_2} \quad (2)$$

where:

$$c = e^{\mu(\alpha_2/2)}\left(T_3 + \frac{\mu a}{1+\mu^2}\sin\left(\frac{\alpha_2}{2}\right)\right)$$

RESULTS:

Results of the formulation for the friction at a crossover region are reflected through the following examples.

Uniformly Distributed Load

For the uniformly distributed load case, the variations of angle $\alpha = \alpha_1 + \alpha_2 + \alpha_3$ as a function of the ratio of T_1/T_4, for α_2 = 0.0°, 30°, 45°, 60°, and 75°, are depicted in *Figure 2*, where r = 1 mm, F_i = 500 N, μ = 0.4, and ω = 5x10^5 N/m. As shown in *Figure 2,* both increasing α and increasing α_2 from the basic solution α_2 = 0 (simple case) to α_2 = 75° increase the yarn tension ratio T_1/T_4. *Figure 2* also reveals that the T_1 tension could reach as high as 3.5 times T_4, which is a significant ratio.

Cosine-shaped Distributed Load

Similarly, for the cosine-shaped distributed load case, the variations of angle $\alpha = \alpha_1 + \alpha_2 + \alpha_3$ as a function of the ratio of T_1/T_4 , for α_2 = 0.0°, 30°, 45°, 60°, and 75°, are depicted in *Figure 3*, where r = 1 mm, F_i = 500 N , a = 1000 N, μ = 0.4 and ω = 5x10^5 N/m. As shown in *Figure 3*, both increasing α and increasing α_2 from the basic solution (simple case, α_2 = 0) to α_2 = 75° increase the yarn tension ratio T_1/T_4. *Figure 3* reveals that the T_1 tension could reach as high as 4.5 times T_4. This increase is more than that of the uniform load case of *Figure 2*.

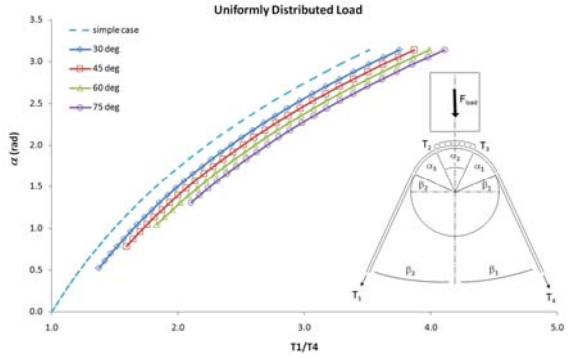

FIGURE 2. Ratio of T_1/T_4 as a Function of α for α_2 = 0.0°, 30°, 45°, 60°, and 75° for Uniformly Distributed Load.

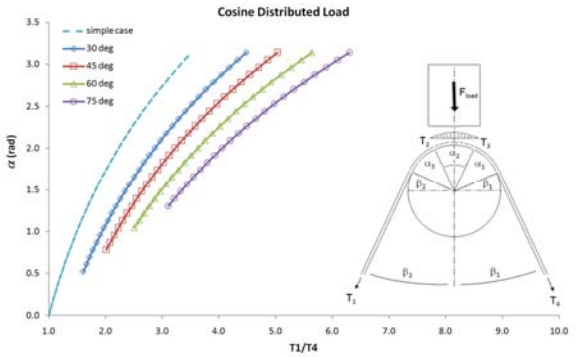

FIGURE 3. Ratio of T_1/T_4 as a Function of α for α_2 = 0.0°, 30°, 45°, 60°, and 75° for Cosine-Shaped Distributed Load.

Figure 2 and 3 reveal that the input tension T_1 of a single crossover region is more than double the output tension T_4, even for small values of angle α_2; that is, to pull a yarn through several crossover regions requires significant force. In addition, the ratio of T_1/T_4 also increases as angle α increases indicating that the yarn pullout force in high crimp content (HCC) yarns is more than that of the low crimp content (LCC) yarns.

YARN PULLOUT FORCES

The weaving architecture of a fabric plays an important role in energy absorbability of the fabric. In addition to unbalanced yarn density ratios, woven fabrics generally have different crimp contents in the warp and weft directions—higher crimp content (HCC) in the warp direction and lower crimp content (LCC) in the weft direction. In *Figure 4*, distance h and t are the distances between the centerlines of adjacent crossover regions in the HCC and LCC directions, respectively. These distances are important parameters in plain-woven fabric architectures and are related to the crimp content and crimp ratio of the fabric, and are therefore related to

the mechanical system properties of the fabric. Through a simple geometric relationship, one can show that a small change in h and/or t, the crimp content and the mechanical properties of the fabric change significantly. The results (not shown due to obvious outcome) established that angle α sharply increased as h and t, the two distances between adjacent yarns in HCC and LCC directions, respectively, were decreased.

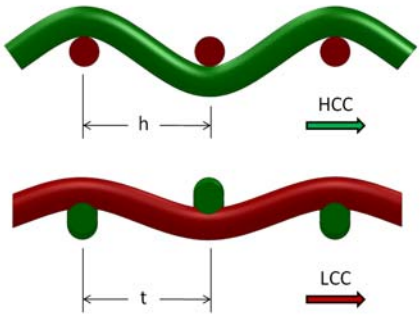

FIGURE 4. Distance Between the Centerlines of Adjacent Crossover Regions in the HCC and LCC Directions.

Two dominant mechanisms of energy absorbability in woven fabrics subjected to low- velocity-projectile impacts are yarn stretching and yarn migration. These mechanisms are related to the force required to pull a yarn out from the fabric and to migrate (push) a yarn away from neighboring crossover regions. If the fabric is made of low-elastic modulus or staple fibers, such as cotton, the pullout force is mainly governed by elastic deformation and elongation of the yarn—the focus of several investigations in which yarn pullout forces from plain-woven cotton fabrics were measured.[11-13] On the other hand, if the fibers of a woven fabric are of high-elastic modulus, continuous fibers, such as Kevlar and Armos aramid, then the pullout force is dominated by the crimp interchange and friction over the crossover regions. Martinez et al.[14] investigated the force required to completely pull out a single Kevlar yarn from a fabric, and Bazhenov[15] investigated the force required to pull out a single Armos aramid yarn from a fabric. Shockey et al.[16] devised an improved pullout test in which the fabric was clamped along its transverse edges.

The analytical formulation of yarn pullout force is of particular interest because it is related to the yarn migration and ballistic protection levels. In the present analysis, the fibers were assumed to be continuous with a high modulus of elasticity and, therefore, the elastic strains in the yarns were neglected. The pullout test is, therefore, largely governed by the frictional phenomenon at the crossover regions. Two cases were considered; namely one with a projectile load and one without a projectile load.

Yarn Pullout Forces Without Projectile Load

Consider a swatch of plain-woven fabric constructed of n number of HCC yarns in the warp direction and n number of LCC yarns in the weft direction; that is, there are nxn number of crossover regions. Assume that the LCC yarns are fixed at both ends and that they remain fixed at a crossover region as an HCC yarn is pulled out from the fabric as shown in *Figure 5*.

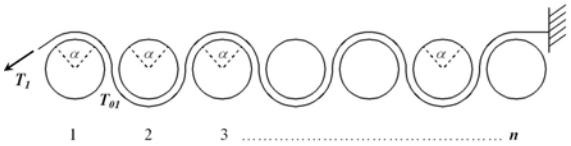

FIGURE 5. n Number Over and Under Crossover Regions for an HCC Yarn.

When an HCC yarn is pulled by a tension T_1, it has n number of over and under crossover regions as shown in *Figure 5*. Based on the weaving architecture and the distance between two adjacent yarns, the contact angle is α at every crossover region.

Denoting the pullout tension as T_1 and the yarn tension on the n^{th} (last) crossover region as T_n, the ratio of the first and the last tensions is:

$$\frac{T_1}{T_n} = e^{\mu n \alpha} \tag{3}$$

Figure 6(a) shows the ratio $Q = T_1/T_n$ as a function of the number of crossover regions n for different contact angles α, and *Figure 6(b)* shows the ratio $Q = T_1/T_n$ as a function of the different values of the coefficient of friction μ. Note that μ varies between 0.1 and 0.4. As *Figures (6a, 6b)* reveal, the ratio Q exponentially increases as the number of crossover regions increases for both cases.

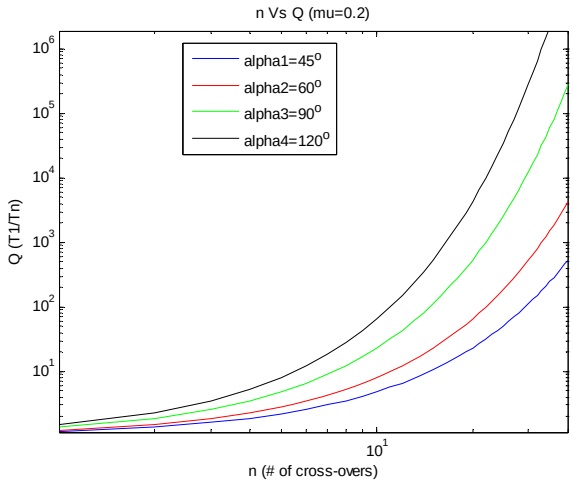

FIGURE 6(a) Ratio $Q = T_1/T_n$ as a Function of n for Different Values of α.

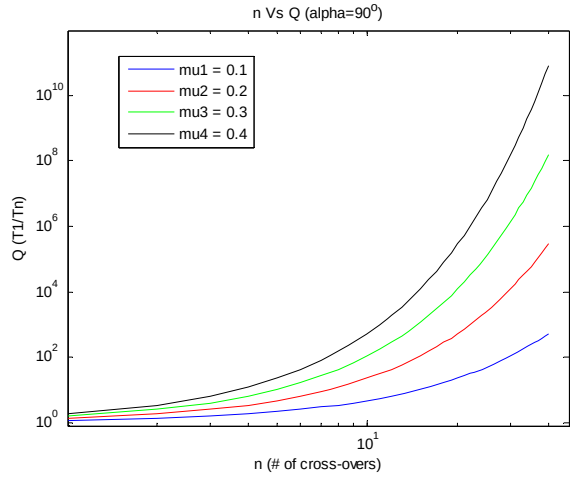

FIGURE 6(b) Ratio $Q = T_1/T_n$ as a Function of n for Different Coefficient of Friction Values.

Yarn Pullout Forces With Projectile Load

For a crimp-imbalanced, plain-woven fabric, the superior section of the yarns at crossover regions will not lie on the same plane; therefore, when a projectile contacts the fabric, contact is established at every other crossover region as shown in *Figure 7*.

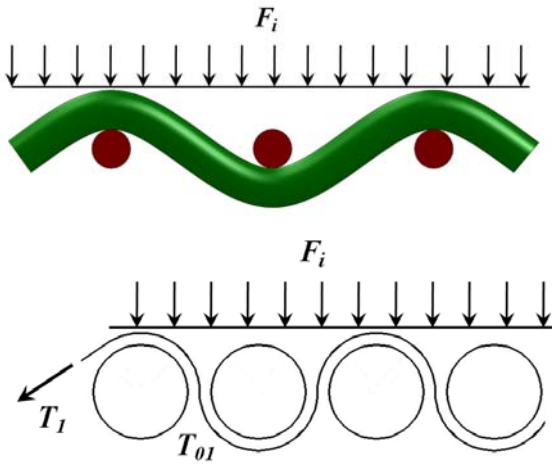

FIGURE 7. Pattern Showing Projectile Contact at Every Other Crossover Region in a Crimp-Imbalanced Architecture.

The equation for the yarn tension, therefore, varies from one crossover region to the next. For example, consider only 10 crossover regions, where five (every other) crossover regions establish contact with the projectile. Denoting the tension on the outside of the 10th crossover region as T_{10}, one can calculate the pullout tension T_1 on the first crossover region, as shown in Eq. (4).

The equation for each of the nine considered crossover regions is given in Eq. (4a - 4d). Solving these coupled equations, the ratio of T_1/T_{10} can be calculated. Consequently, for n number of crossovers, one can determine the ratio of T_1/T_n following the sequence described in Eq. (4a - 4d).

Crossover Region 1: $$\frac{T_1 + \frac{F_i}{\alpha}}{T_2 + \frac{F_i}{\alpha}} = e^{\mu\alpha} \qquad (4a)$$

Crossover Region 2: $$\frac{T_2}{T_3} = e^{\mu\alpha} \qquad (4b)$$

Crossover Region 8: $$\frac{T_8}{T_9} = e^{\mu\alpha} \qquad (4c)$$

Crossover Region 9: $$\frac{T_9 + \frac{F_i}{\alpha}}{T_{10} + \frac{F_i}{\alpha}} = e^{\mu\alpha} \qquad (4d)$$

EXAMPLE

The following examples are given to demonstrate the variations of the yarn pullout force in a fabric. In these examples the restrained force, T_n, which is the tension created by the projectile, is needed. This force is estimated as follows.

Consider a fabric swatch of size *LxL* (for example, 40x40 mm^2) where its boundaries are clamped as shown in *Figure 8(a)*. When a low-velocity projectile impacts the center of the fabric in the region of 10x10 mm^2 the fabric deflects globally by amount δ as is shown in *Figure 8(b)*.

(a)

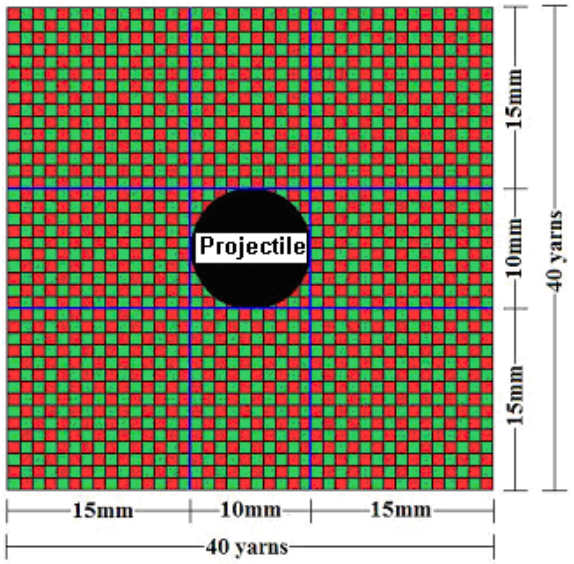

(b)

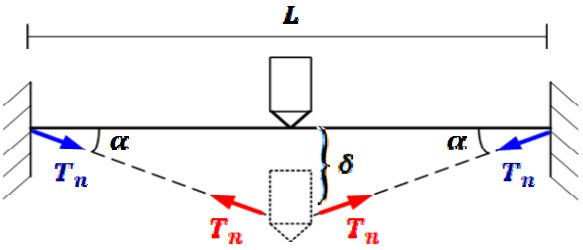

FIGURE 8. (a) Top View of the Fabric with Dimensions and Location of Projectile, (b) Schematic Cross-Sectional View of Fabric Showing Global Deflection δ and Tension T_n

Thus, the tension in the i^{th} yarn, T_{ni}, is $T_{ni} = F_i/(2\sin\alpha) = F_i/(2(2\delta/L)) = F_iL/4\delta$, where F_i is the projectile's impact force on the yarn. In an extreme case, if the fabric with n number of yarns arrests the projectile, then, the work-energy relationship is $F_i\delta n = 1/2mV^2$. To estimate the range of the projectile force F_i and the yarn tension T_{ni}, the following assumptions are made: (1) the projectile velocity is 300 m/sec, (2) the projectile weight is 10 grams (0.01 kg), (3) the projectile is shaped as a right circular cylinder with cross-sectional diameter of 10 mm, (4) the coefficient of friction of yarns at the crossover regions is 0.1 to 0.4, and (5) the fabric global deflection, δ, due to the projectile contact is approximately 10% of the fabric length. Based on these assumptions the average projectile force on each yarn, F_i, is 70 N. Since the assumptions may not reflect the actual impact force, a wider range of force such as 40 N to 100 N is considered. For this range of impact force, the tension of the yarn varies between 175 N to 250 N. To cover a wider range of yarn tension, the range of T_i = 100 N to 500 N is used. The results of this case are shown in *Figure 9* where the pullout force T_1 is depicted as a function of α for different values of T_{10} (ranging from 100 N to 500 N) and contact force of F_i = 100 N. Note that increasing α, which increases the crimp contents in the HCC yarns, exponentially increases the pullout force. Similar curves and variations as in *Figure 9* were observed when the contact force F_i was changed.

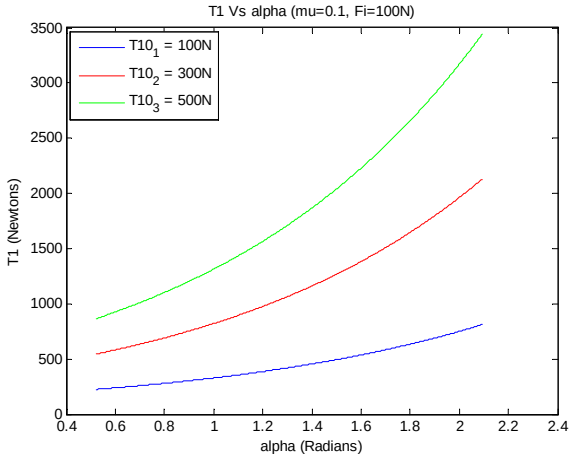

FIGURE 9. Yarn Pullout Force T_1 as a Function of α, for Different Values of T_{10} where F_i = 100 N.

YARN MIGRATION FORCES:

During a low-velocity impact in which a projectile contacts a plain-woven fabric, deflection of the fabric plane occurs. This creates tension in the primary yarns which leads to migration of these yarns away from the impact zone. That is, the primary yarns are forced to migrate (move or slide) away from the point of impact along the direction perpendicular to their longitudinal axes over the crossing yarn family as shown in *Figure 10(b)*. This migration phenomenon

results from the limited frictional force (that is, limited slip resistance) developed at the crossover regions.

The primary yarn migrations lead to the formation of openings between adjacent yarns, which permit the projectile to penetrate the fabric without yarn failure. (Recall the invoked assumption that yarn failures are not permitted in the current analysis.) Note by definition that the LCC yarns have less crimp content than the HCC yarns.

(a)

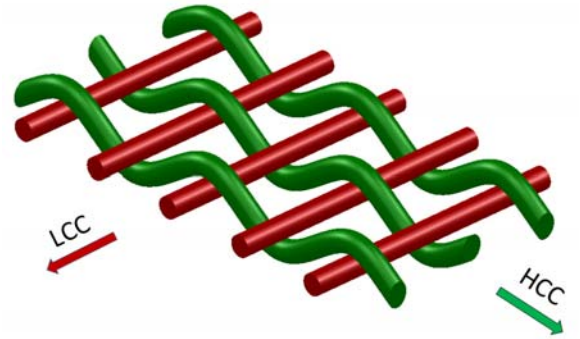

(b)

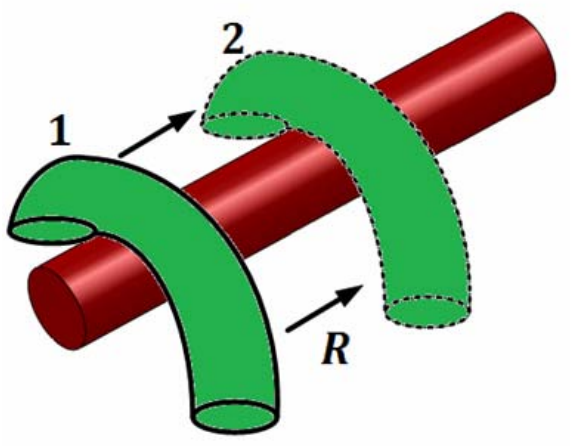

FIGURE 10. (a) Woven Fabric with HCC Yarns Aligned in the Weft Direction and LCC Yarns Aligned in the Warp Direction and (b) Migration Phenomenon.

Migration Force Without Projectile Load

Let the migration force on the yarns in the HCC or the LCC direction be denoted by *R*. The free-body diagram of a single crossover region is shown in *Figure 11*.

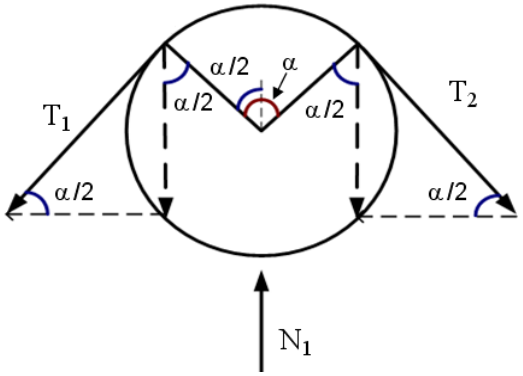

FIGURE 11. Free-Body Diagram of a Single Crossover Region

Using static equilibrium, the migration force of a single yarn R_1 (in the direction perpendicular to the page) can be derived as, $R_1 = \mu(T_1 + T_2)\sin(\alpha/2)$. Consider a yarn that spans *n* crossover regions: the general formula for the total migration force *R* for the n^{th} crossover region is given by,

$$R = \sum_{i=1}^{n-1} R_i = \mu \sin\left(\frac{\alpha}{2}\right)\left[2\sum_{i=1}^{n} T_i - \left(T_1 + T_{n+1}\right)\right] \qquad (5)$$

Substituting $T_i = (T_{i+1})e^{\mu\alpha_i}$, and repeating this process, one can arrive at:

$$R = \mu \sin\left(\frac{\alpha}{2}\right)\left[T_n \times 2 \times \frac{e^{\mu\alpha(n+1)} - 1}{e^{\mu\alpha} - 1} - T_n\left(1 + e^{\mu\alpha(n)}\right)\right] \qquad (6)$$

Consider now, for example, a yarn spanning 10 crossover regions. The equation for the migration force is then given by Eq. (7). To make the force nondimensional, T_{10} is factored out and the results are given in terms of $P = R/T_n$. *Figure 12* depicts the variation of *P* with respect to the number of crossover regions *n* for various values of α and coefficients of friction μ. As shown in *Figure 12*, increasing the number of crossovers and α (that is, higher crimp content) exponentially increases the migration force—similar to the pullout force described in the previous section.

$$P = R / T_{10}$$

$$P = \mu \sin\left(\frac{\alpha}{2}\right)\left[2 \times \frac{e^{\mu\alpha(11)} - 1}{e^{\mu\alpha} - 1} - \left(1 + e^{\mu\alpha(10)}\right)\right] \qquad (7)$$

(a)

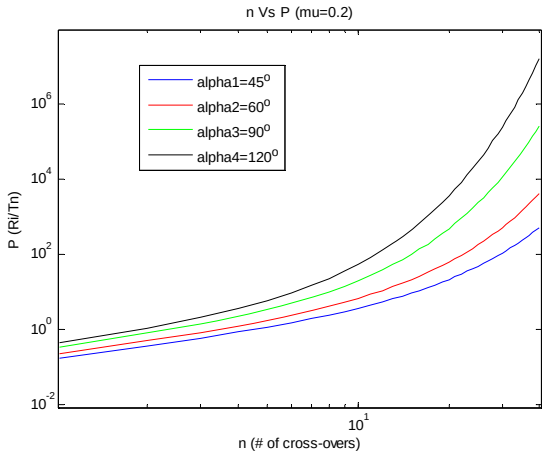

(b)

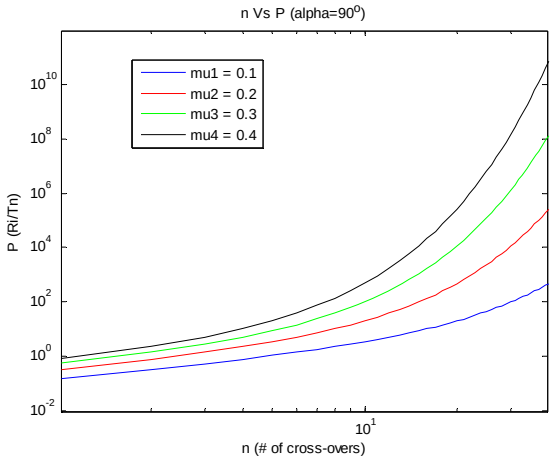

FIGURE 12. (a) Migration Force Ratio P vs. Number of Crossover Regions (for μ = 0.2, α = 45°, 60°, 90°, 120°) and (b) Migration Force Ratio P vs. Number of Crossover Regions (for μ = 0.1, 0.2, 0.3, 0.4).

Migration Force With Projectile Load

The free-body diagram of a single crossover region in a crimp-imbalanced, plain-woven architecture is shown in *Figure 13*. Using the equilibrium of the crossover region, the contact migration force R_1 can be derived as:

$$R_1 = \mu(T_1 + T_2)\sin\left(\frac{\alpha}{2}\right) + \mu F_i. \qquad (8)$$

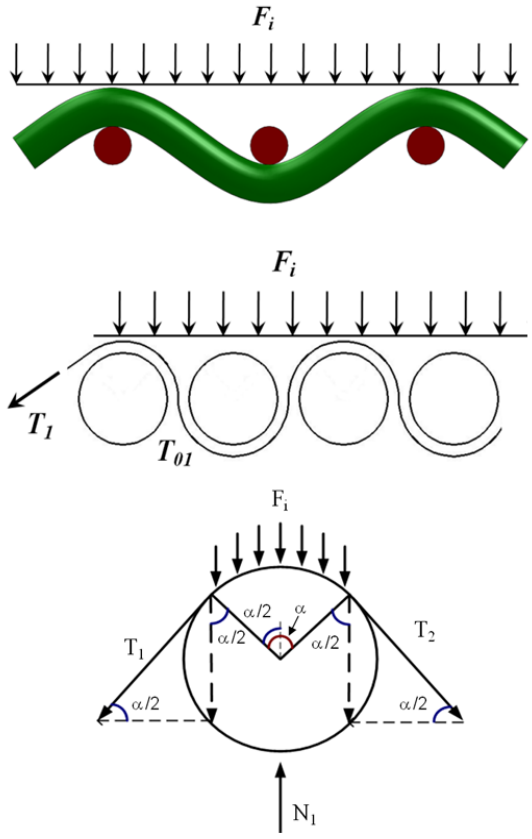

FIGURE 13. Schematic and Free-Body Diagrams of Crossover Regions in a Crimp-Imbalanced Architecture.

As shown in the case of *Figure 13*, there is a noncontact crossover region adjacent to the contact crossover region, thus the migration force for the noncontact region is, $R_2 = \mu(T_2 + T_3)\sin\left(\frac{\alpha}{2}\right)$.

The equations for R_1 and R_2 can be expanded for n crossover regions. Therefore, for a yarn with n crossover regions, the migration force is:

$$R = \mu\sin\left(\frac{\alpha}{2}\right)\times T_n\left[2\times\frac{e^{\mu\alpha(n+1)}-1}{e^{\mu\alpha}-1} - \left(1+e^{\mu\alpha(n)}\right)\right] + \frac{(n-1)}{2}\mu F_i \qquad (9)$$

Similar to the previous example, consider 10 crossover regions. The variation of the migration force R as a function of α, for different values of T_{10} and different values of external force F_i is depicted in *Figure 14*. As shown in *Figure 14*, increasing α (that is, higher crimp content) significantly increases the migration force—similar to the pullout force described in the previous section.

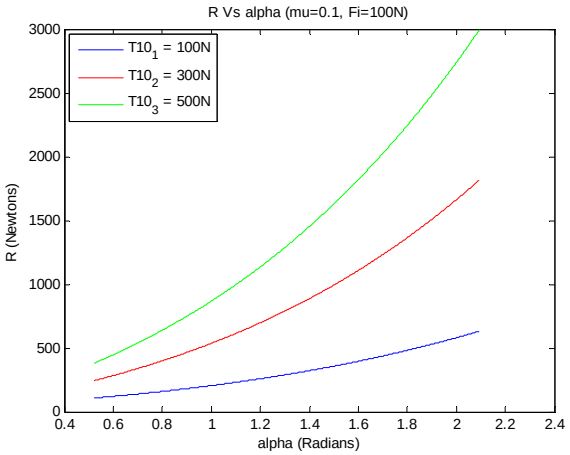

FIGURE 14. Migration Force R for Different Values of T_{10} and the external load of F_i = 100 N

YARN PULLOUT AND MIGRATION FORCES REQUIRED TO FULLY PENETRATE A PLAIN-WOVEN FABRIC

When a projectile contacts a woven fabric, relative motions of the primary yarns occur that lead to crimp interchange, yarn stretch, yarn pullout, fabric shearing, and yarn migration. For projectiles with conical leading edges, the projectile's geometry is even more capable of pushing aside yarns in its path, which eventually leads to the formations of openings within the fabric sufficiently sized to enable penetration to occur without yarn fractures. To create a sufficiently sized opening, yarns of each family migrate along their relative orthogonal directions. In this analysis, it is assumed that the yarns do not fail, rather the projectile creates an opening of diameter *D*.

The pullout force of a yarn is denoted by T_i and its migration force is denoted by R_i. To derive the total force on the yarns, a sequence of families of yarns were considered. First, consider the 2x2 representation of plain-woven yarns shown in *Figure 15*.

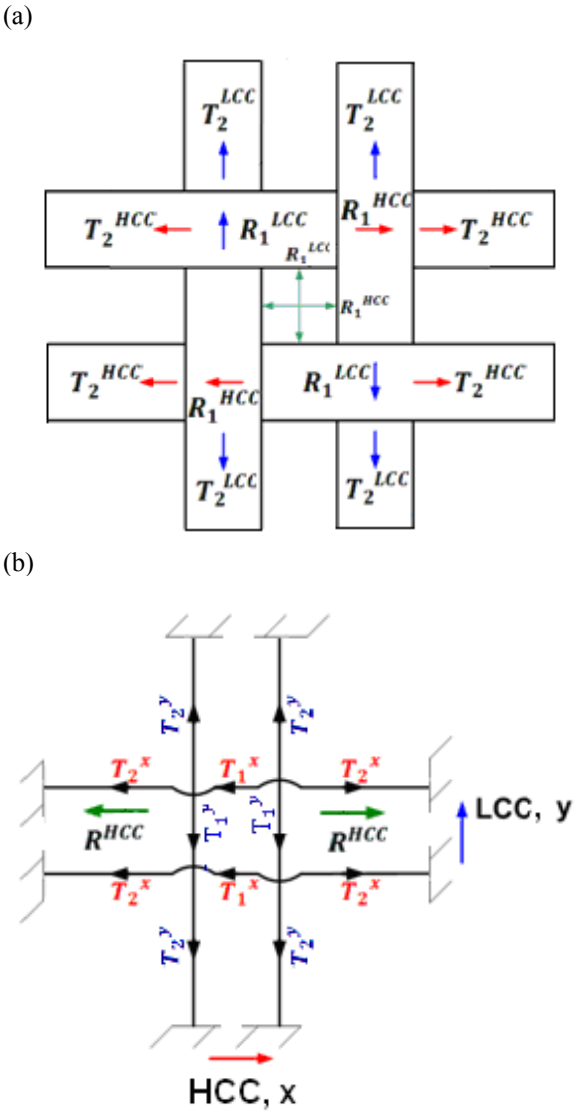

FIGURE 15. (a) Pullout (T_i) and (b) Migration (R_i) Forces in a 2x2 Plain-Woven Yarn Fabric.

Note that, along the HCC yarn direction, the contact angle α is denoted by α_x or α_{HCC}; similarly, along the LCC yarn direction, the contact angle α is denoted by α_y or α_{LCC}. Pullout tensions, T_i, associated with the HCC and LCC directions are denoted by $T_x = T_{HCC}$ and $T_y = T_{LCC}$, respectively. Likewise, the migration forces, R_i, associated with the HCC and LCC directions are denoted by $R_x = R_{HCC}$ and $R_y = R_{LCC}$, respectively. Note that T_{ix} or T_{iy} can be determined by using the pullout Eq. (4a - 4d) therefore, the equations for T_{ix} or T_{iy} are not repeated here.

The 2x2 plain-woven yarn fabric, the migration force in the x-direction (HCC direction) can be derived as:

$$\begin{aligned} R_x = R_{HCC} &= 4R_{1x} \\ R_x = R_{HCC} &= 4\mu(T_{1x} + T_{2x})Sin(\alpha/2) \\ R_x = R_{HCC} &= 4\mu\left(T_{2x}e^{\mu\alpha_x} + T_{2x}\right)\sin\left(\frac{\alpha_x}{2}\right) \\ R_x = R_{HCC} &= 4\mu\left(1 + e^{\mu\alpha_x}\right)T_{2x}\sin\left(\frac{\alpha_x}{2}\right) \end{aligned} \quad (10)$$

Similarly, the migration force in the y-direction (LCC direction) can be derived as:

$$R_y = R_{LCC} = 4\mu\left(1 + e^{\mu\alpha_y}\right)T_{2y}\sin\left(\frac{\alpha_y}{2}\right) \quad (11)$$

When considering a 4x4 plain-woven yarn fabric as depicted in *Figure 16*, the migration force in the x-(HCC) direction and y-(LCC) direction can be derived as:

$$R_x = R_{HCC} = 8\mu(T_{1x} + 2T_{2x} + T_{3x})\sin\left(\frac{\alpha_x}{2}\right)$$

and (12)

$$R_y = R_{LCC} = 8\mu(T_{1y} + 2T_{2y} + T_{3y})\sin\left(\frac{\alpha_y}{2}\right)$$

Note, if the fabric is also subjected to projectile impact force, F_i, then the term $n\mu F_i$ should be added to Eq. (10), Eq. (11) and Eq. (12). For the 2x2 and 4x4 plain-woven yarn cases considered, the pullout forces T_{ix} or T_{iy} can be determined by using Eq. (4a - 4d). Note also that the difference between R_x and R_y depends upon the appropriate contact angle used; α_x (i.e.; α_{HCC}) or α_y (i.e.; α_{LCC}).

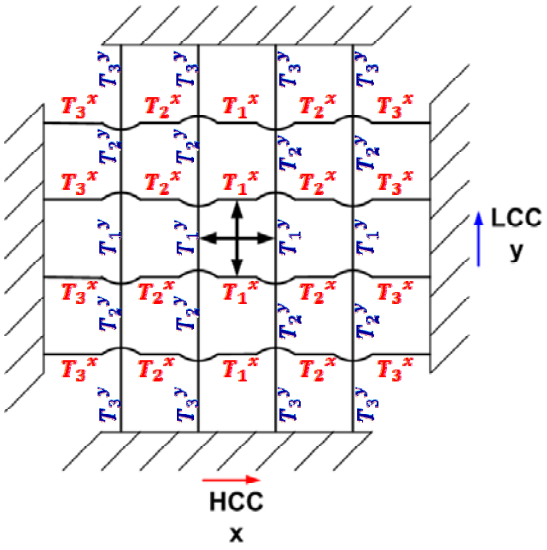

FIGURE 16. Pullout (T_i) and Migration (R_i) Forces in a 4x4 Plain-WovenYarn Fabric.

To quantify the values of migration force R, consider the 8x8 plain-woven yarn fabric case as shown in *Figure 17*. For this case, the migration force in the x-(HCC) direction and y-(LCC) direction can be derived as:

$$R_x = R_{HCC}$$

$$R_x = 16\mu\sin\left(\frac{\alpha_x}{2}\right)\left(T_{1x} + 2T_{2x} + 2T_{3x} + 2T_{4x} + T_{5x}\right) \quad (13)$$

and

$$R_y = R_{LCC}$$

$$R_y = 16\mu\sin\left(\frac{\alpha_y}{2}\right)\left(T_{1y} + 2T_{2y} + 2T_{3y} + 2T_{4y} + T_{5y}\right) \quad (14)$$

respectively. The results of R_x and R_y as a function of α for different T_5 (the last pullout force or the restrained tension) and for F_i =40 N are shown in *Figure 18*.

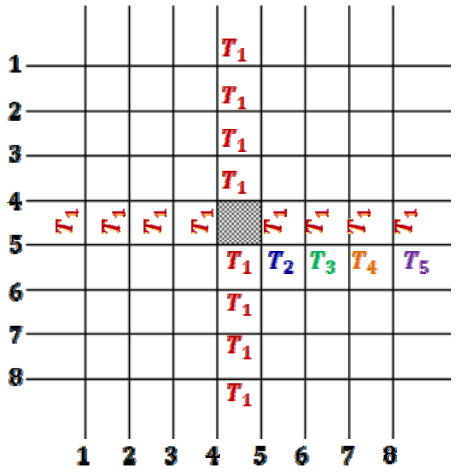

FIGURE 17. 8x8 Plain-Woven Yarn Fabric.

(a)

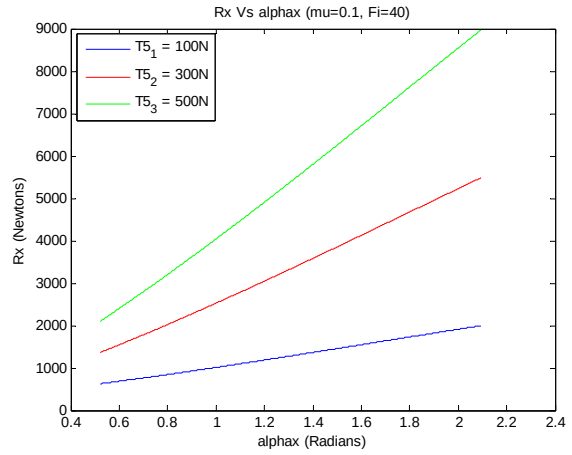

(b)

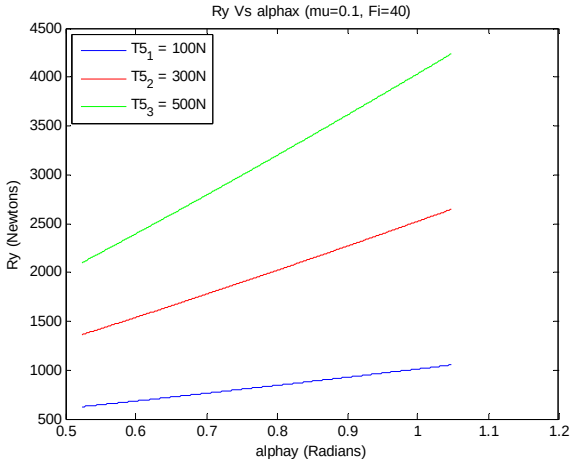

FIGURE 18. (a) R_x Migration Forces As a Function of α for Different Values of T_5 and $F_i = 40$ and (b) R_y Forces As a Function of α for Different Values of T_5 and $F_i = 40$

General Formulation For Plain-Woven Fabric Of *nxn* Yarns

The equation for the migration force of a fabric containing a *nxn* yarns in the x-direction R_x can be derived as:

$$R_x = 2n\mu \sin\left(\frac{\alpha_x}{2}\right)\left[2\sum_{i=1}^{n+1} T_{ix} - \left(T_{ix} + T_{(n+1)x}\right)\right] + n\mu Fi \quad (15a)$$

and in the y-direction R_y as:

$$R_y = 2n\mu \sin\left(\frac{\alpha_y}{2}\right)\left[2\sum_{i=1}^{n+1} T_{iy} - \left(T_{1y} + T_{(n+1)y}\right)\right] + n\mu Fi \quad (15b)$$

where the values of T_i in Eq. (15a) and Eq. (15b) are derived from the following equations, (as developed in previous sections.)

In the x-direction,

$$\frac{T_n + \dfrac{F_i}{\alpha_x}}{T_{n+1} + \dfrac{F_i}{\alpha_x}} = e^{\mu\alpha_x}$$

and in the y-direction, (16)

$$\frac{T_n + \dfrac{F_i}{\alpha_y}}{T_{n+1} + \dfrac{F_i}{\alpha_y}} = e^{\mu\alpha_y}$$

The relationship between the first and the last tension for the n^{th} crossover region is given by

$$\frac{T_1 + \dfrac{F_i}{\alpha}}{T_{n+1} + \dfrac{F_i}{\alpha}} = e^{\mu n\alpha} \quad (17)$$

where the angle α can be replaced by α_x or α_y.

ENERGY ABSORPTION AND THE PROJECTILE RESIDUAL VELOCITY

When a projectile with a conically shaped leading edge contacts a fabric at low velocity, the plane of the fabric deflects causing initial tension, crimp interchange, yarn pullout, yarn migration, and fabric shearing. As the projectile continues to deflect the fabric plane, the leading edge simply creates an

opening between yarn families and, finally, penetration occurs through the opening. The work done by yarn pullout and migration during impact is equal to the change in the projectile's kinetic energy. Note that, heat generation and the elastic strain energy of the yarns were neglected. Because energy is conserved, the work done by the impact force on the fabric is equal to the change in kinetic energy of the projectile (i.e.; a function of the velocity change in the projectile). Part of the kinetic energy of the projectile is absorbed by the initial tension and deflection of the fabric plane. The majority of the energy, however, is absorbed by the yarn pullout and migration processes. Note that, as the projectile creates an opening within the fabric, both the HCC (warp direction) and LCC (weft direction) yarns are subjected to pullout and migration forces, as shown in *Figure 19*.

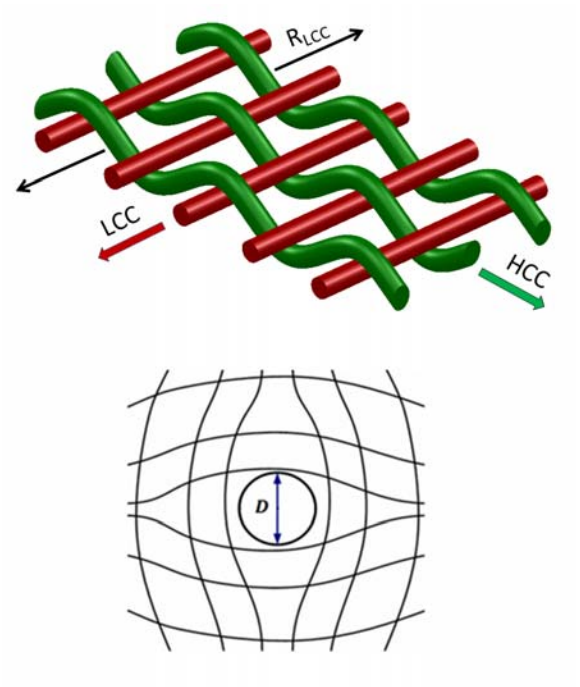

FIGURE 19. Pullout and Migration Forces in both HCC and LCC Yarns

For this analysis, consider a swatch of plain-woven fabric consisting of *n*x*n* number of crossover regions that is impacted by a projectile (see *Figure 8a*). To quantify the residual velocity of the projectile, the following assumptions were made:

1. The fabric architecture is plain-woven.
2. The fabric edges are clamped.
3. The yarns have a circular cross-section with diameter equal to 1.0 mm.
4. Yarn-to-yarn coefficient of friction varies from μ=0.1 to 0.4.
5. Yarns do not fail during impact.
6. α varies from 30° to 120° for HCC (as α_x) and from 30° to 60° for LCC (as α_y).
7. Tension at the clamped edge of the fabric is T_{in}=100 N to 500 N.
8. Projectile diameter is 10 mm.
9. Projectile weight is 10 g.
10. Initial velocity of the projectile is V_1=300 m/sec.
11. Cross-sectional changes due to yarn compactions at the crossover regions are negligible.
12. Yarns are assumed to be constructed of high-modulus elastic fibers, thus, the elastic strain of the yarn is neglected.

Assume that the HCC yarns migrate outward from the impact zone by D_x and are pulled out along the x-direction by amount Δ_x; likewise, assume that the LCC yarns migrate outward from the impact zone by D_y and are pulled out along the y-direction by amount Δ_y. The work W required to create an opening within the *n*x*n plain*-woven fabric is equal to the work done by the pullout and migration forces in the x- and y-directions through distances D_x and Δ_x , and is:

$$W = \left(R_x D_x + R_y D_y\right) + 2n\left(T_{1x}\Delta_x + T_{1y}\Delta_y\right) \qquad (18)$$

Because energy is conserved (i.e.; elastic strain energy of the yarns is neglected), the total work done by the yarn pullout and yarn migration forces was equated to the change in kinetic energy of the projectile. Therefore, the residual velocity, V_2, of the projectile, can be computed as:

$$W = \frac{1}{2} m\left(V_2^2 - V_1^2\right) \qquad (19)$$

RESULTS

To quantify the residual velocity of a projectile, consider an example of a plain-woven fabric swatch containing 8x8 yarns as shown in *Figure 17*. Crimp contents in the HCC direction and LCC direction are denoted as $\alpha_x = \alpha_{HCC}$ and $\alpha_y = \alpha_{LCC}$, respectively. Therefore, crimp imbalance is defined as $\alpha_z = \alpha \dfrac{\alpha_x}{\alpha_y} = \dfrac{\alpha_{HCC}}{\alpha_{LCC}} > 1$. The total work done by the pullout and migration forces as a function of α_z, for different values of the tension T_5 (the tension at the swatch outer edge) is shown in *Figure 20*.

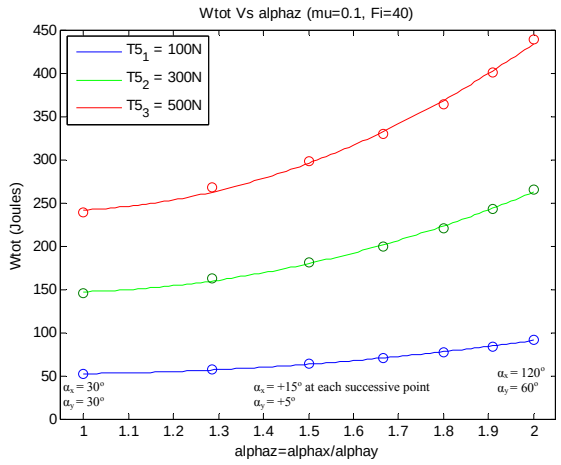

FIGURE 20: Work Done by Pullout and Migration Forces as a Function of $\alpha_z = \frac{\alpha_x}{\alpha_y}$ for Different Values of T_5

Finally, the projectile residual velocity V_2 is shown in *Figure 21*. As shown in *Figure 21*, V_2 reduces when the angle $\alpha_z = \frac{\alpha_x}{\alpha_y}$ is increased; that is, increased crimp content of the HCC yarns results in greater energy absorption leading to improved ballistic protection levels of the fabric.

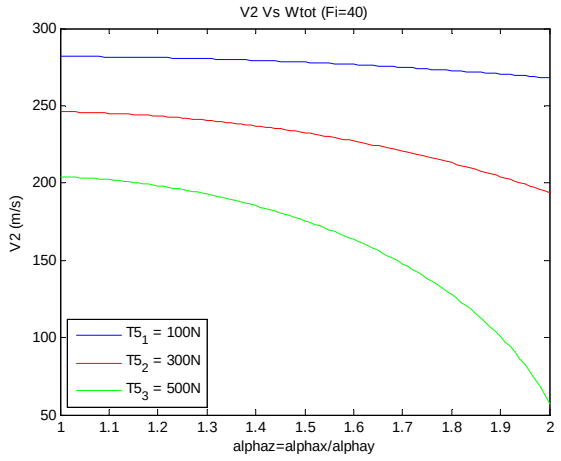

FIGURE 21: Projectile's Residual Velocity V_2 as a Function of $\alpha_z = \frac{\alpha_x}{\alpha_y}$ for Different Values of T_5

SUMMARY AND CONCLUSIONS

Plain-woven fabrics have traditionally been utilized in flexible protection systems because of their combined lightweight and high-strength characteristics. Furthermore, their heterogeneous constructions provide multiple energy absorption mechanisms present at both the yarn and fabric scales enabling them to efficiently and uniquely resist ballistic impacts. The preliminary ballistic experiments revealed that high crimp content fabrics have better ballistic performance than low crimp content fabrics. The primary objective of this research was to analytically investigate and quantify the hypothesis that fabrics constructed with one yarn family having higher crimp content and the other orthogonal yarn family having lower crimp content achieve greater ballistic impact energy absorption. More specifically, this study investigated the mechanism of projectile penetration in plain-woven fabrics and has developed an analytical solution that quantifies the: (1) yarn-yarn friction forces generated during yarn pullout, (2) frictional forces generated by yarn migration, (3) work required to create an opening in the fabric and (4) residual velocity of the projectile.

For a single crossover region, two types of distributed loads were considered, namely a uniform distribution and a cosine-shaped distribution. For each case, the ratio of input tension/output tension (T_1/T_4) was analytically derived. The results revealed that tension T_1 could exceed 3.5 times that of T_4. This increase was even greater for the cosine-shaped distributed load case. In addition, it was found that an increase in the contact angle also increases the (T_1/T_4) ratio. Note that, in all the analyses described in the present paper, the fibers were assumed to have a high modulus of elasticity; thus the elastic strain of the yarn was neglected.

The architecture of woven fabrics was also studied. The centerline distances between adjacent crossover regions as a function of contact angle α was analyzed. The results established that angle α sharply increased as h and t (the distances between adjacent crossover regions in the HCC and LCC directions) respectively, decreased.

As one of the mechanisms of energy absorbability in plain-woven fabrics, the forces associated with yarn pullout, T_i, for n number of crossover regions with and without the projectile forces were derived. The results revealed that the ratio of yarn tensions at both ends (T_i/T_{ni}) exponentially increased with an increase in the coefficient of friction μ, angle α, and the number of crossover regions.

By using a realistic example of a projectile velocity of 300 m/sec and projectile weight of 10 g, the range of the impact force on each yarn F_i was approximated

to be 70 N, (based on the 10% deflection of the fabric). Since the assumptions may not reflect an actual impact force, a wider range of the force, 40 N to 100 N was considered. Therefore, the range of tension T_{ni} at the clamped edge was estimated to be between 100 N to 500 N. The ranges of F_i and T_{ni} were used for the calculations of the yarn pullout and yarn migration forces studied in this report. The results of the pullout analysis revealed that, for a given T_{ni}, the tension exponentially increased as angle α increased.

In addition to the yarn pullout force, the yarn migration forces, R_i, were studied. This phase of the investigation was particularly salient because it demonstrated the significant effect that projectiles with conical leading edges can have on penetration resistance of plain-woven fabrics. Specifically, a projectile with a conical leading edge deflects the fabric and, in doing so, causes greater migration of the primary yarns away from the impact zone—creating openings that can easily lead to through-penetration. Yarn migration forces, for cases with and without projectile impact, were derived. The results revealed that P, the ratio of R_i/T_{ni}, exponentially increased with increases in coefficient of friction μ, contact angle α, and the number of crossover regions n. The same example used for the pullout analysis was used for the yarn migration force analysis. The results of the migration analysis revealed that, for a given T_{ni}, as α increased, the migration force significantly increased.

Plain-woven fabrics can absorb significant kinetic energy from projectile and fragment impacts through a combination of yarn pullout and yarn migration mechanisms. The relationship between the energy absorbed by the yarn migration and the residual velocity of the projectile was developed. It was assumed that the projectile created an opening of diameter D. Then the work done by yarn pullout and yarn migration forces for 2x2, 4x4, and 8x8 woven yarn fabrics cases were derived. In this study, energy transfer due to heat, elastic strain energy, plastic strain energy, and material damping were considered negligible. Thus, the work done by yarn pullout and yarn migration was equated to the change in kinetic energy of the projectile, which was used to compute the residual velocity V_2 of the projectile. The results revealed that V_2 decreased with increasing the ratio of contact angles, $\alpha_z = \frac{\alpha_x}{\alpha_y}$; that is, increased crimp content of the HCC yarns increased the energy absorption level of the fabric.

Finally, the results of this study confirmed that fabrics with high crimp contents absorb greater ballistic impact energies than fabrics with low crimp contents. That is, as the crimp content and yarn-to-yarn contact angle, α, of the crossover regions is increased, the work done by the projectile on the woven fabric is increased, which leads to smaller values of residual velocity V_2. Note that the magnitude of α constituted the crimp content in a given yarn direction. These analyses revealed that woven fabrics constructed of high crimp contents (that is, larger α) absorbed more impact energy than did fabrics with low crimp contents. These conclusions have been confirmed by the numerical analysis described in NUWC-NPT Technical Report 11,957 [6]. Future experimental tests should be pursued for validation of the analyses performed.

REFERENCES:

[1] B. A. Cheeseman and T. A. Bogetti, "Ballistic Impact into Fabric and Compliant-

[2] R. Park and J. Jeng, "Effect of Laminate Geometry on Impact Performance of Aramid Fiber/Polyethylene Fiber Hybrid Composites," *Journal of Applied Polymer Science*, vol. 75, pp. 952 – 959, 2000.

[3] D. Roylance, A. Wilde, and G. Tocci, "Ballistic Impact of Textile Structures,"

[4] D. J. Carr, "Failure Mechanism of Yarns Subjected to Ballistic Impact," *Journal of Materials Science Letters*, vol. 18, no. 7, pp. 585 –588, April 1999.

[5] M. J. Jacob and J. L. Van Dingenen, "Ballistic Protection Mechanisms in Personal Armour," *Journal of Materials Science*, vol. 36, pp. 3137 – 3142, 2001.

[6] P. Cavallaro and A. Sadegh, "Crimp-Imbalanced Protective (CRIMP) Fabrics,"

[7] B. J. Briscoe and F. Motamedi, "The Ballistic Impact Characteristics of Aramid Fabrics: The Influence of Interface Friction," *Wear*, vol. 158, pp. 229 – 247, 1992.

[8] Y. S. Lee, E. D. Wetzel, and N. J. Wagner, "The Ballistic Impact Characteristics of Kevlar Woven Fabrics Impregnated with a Colloidal Shear Thickening Fluid," *Journal of Materials Science*, vol. 38, pp. 2825 – 2833, 2003.

[9] L. Dischler, T. T. Moyer, and J. B. Henson, "Dilatant Powder Coated Fabric and Containment Articles Formed There," U.S. Patent 5,776,839, 1998.

[10] J. Awerbuch and S. R. Bonder, "Analysis of the Mechanics of Perforation of Projectiles in Metallic Plates," *International Journal of Solids and Structures*, vol. 10, pp. 671 – 684, 1974.
[11] S. A. Sebastian, A. I. Bailey, B. J. Briscoe, and D. Tabor, "Effect of a Softening Agent on Yarn Pull-Out Force of a Plain Weave Fabric," *Textile Research Journal*, vol. 56, pp. 604 – 611, 1986.
[12] S. A. Sebastian, A. I. Bailey, B. J. Briscoe, and D. Tabor, "Extensions, Displacements, and Forces Associated with Pulling a Single Yarn From a Fabric," *Journal of Physics D: Applied Physics*, vol. 20, pp. 130 – 139, 1987.
[13] F. Motamedi, A. I. Bailey, B. J. Briscoe, and J. Tabor, "Theory and Practice of Localized Fabric Deformations," *Textile Research Journal*, vol. 59, pp. 160 – 172, 1989.
[14] M. A. Martinez, C. Navarro, R. Cortes, J. Rodriguez, and V. Sanchez-Galvez, "Friction and Wear Behaviour of Kevlar Fabrics," *Journal of Materials Science*, vol. 28, pp. 1305 – 1311, 1993.
[15] S. Bazhenov, "Dissipation of Energy by Bulletproof Aramid Fabric," *Journal of Materials Science*, vol. 32, pp. 4167 – 4173, 1997.
[16] D. A. Shockey, D. C. Erlich, and J. W. Simons, "Improved Barriers to Turbine Engine Fragments: Interim Report III," DOT/FAA/AR-99/8, III, Office of Aviation Research, Federal Aviation Administration, Washington, DC 2001.

AUTHORS' ADDRESSES

Ali M. Sadegh
The City College of
The City University of New York
Mech. Eng.
Convent Ave. and 140th Street
New York, New York 10031
UNITED STATES
212-650-5203

Paul V. Cavallaro
Naval Undersea Warfare Center Division
1176 Howell Street
Newport, RI, 02841
UNITED STATES
401-832-5082
paul.cavallaro@navy.mil